High productivity in hybrid-poplar plantations without isoprene emission to the atmosphere

Russell K. Monson[a,b,1], Barbro Winkler[c], Todd N. Rosenstiel[d,1], Katja Block[c], Juliane Merl-Pham[e], Steven H. Strauss[f], Kori Ault[f], Jason Maxfield[d], David J. P. Moore[g], Nicole A. Trahan[g], Amberly A. Neice[g], Ian Shiach[g], Greg A. Barron-Gafford[h], Peter Ibsen[i], Joel T. McCorkel[j], Jörg Bernhardt[k], and Joerg-Peter Schnitzler[c,1]

[a]Department of Ecology and Evolutionary Biology, University of Arizona, Tucson, AZ 85721; [b]Laboratory of Tree-Ring Research, University of Arizona, Tucson, AZ 85721; [c]Research Unit Environmental Simulation, Institute of Biochemical Plant Pathology, Helmholtz Zentrum München, 85764 Neuherberg, Germany; [d]Department of Biology, Portland State University, Portland, OR 97207; [e]Research Unit Protein Science, Helmholtz Zentrum München, 85764 Neuherberg, Germany; [f]Department of Forest Ecosystems and Society, Oregon State University, Corvallis, OR 97331; [g]School of Natural Resources and the Environment, University of Arizona, Tucson, AZ 85721; [h]School of Geography and Development, University of Arizona, Tucson, AZ 85721; [i]Department of Botany and Plant Science, University of California, Riverside, CA 92507; [j]Biospheric Sciences Laboratory, NASA Goddard Space Flight Center, Greenbelt, MD 20771; and [k]Institute for Microbiology, Ernst-Moritz-Arndt University, 17487 Greifswald, Germany

Edited by Astrid Kiendler-Scharr, Forschungszentrum Jülich GmbH, Jülich, Germany, and accepted by Editorial Board Member Ravi R. Ravishankara November 28, 2019 (received for review July 17, 2019)

Hybrid-poplar tree plantations provide a source for biofuel and biomass, but they also increase forest isoprene emissions. The consequences of increased isoprene emissions include higher rates of tropospheric ozone production, increases in the lifetime of methane, and increases in atmospheric aerosol production, all of which affect the global energy budget and/or lead to the degradation of air quality. Using RNA interference (RNAi) to suppress isoprene emission, we show that this trait, which is thought to be required for the tolerance of abiotic stress, is not required for high rates of photosynthesis and woody biomass production in the agroforest plantation environment, even in areas with high levels of climatic stress. Biomass production over 4 y in plantations in Arizona and Oregon was similar among genetic lines that emitted or did not emit significant amounts of isoprene. Lines that had substantially reduced isoprene emission rates also showed decreases in flavonol pigments, which reduce oxidative damage during extremes of abiotic stress, a pattern that would be expected to amplify metabolic dysfunction in the absence of isoprene production in stress-prone climate regimes. However, compensatory increases in the expression of other proteomic components, especially those associated with the production of protective compounds, such as carotenoids and terpenoids, and the fact that most biomass is produced prior to the hottest and driest part of the growing season explain the observed pattern of high biomass production with low isoprene emission. Our results show that it is possible to reduce the deleterious influences of isoprene on the atmosphere, while sustaining woody biomass production in temperate agroforest plantations.

oxidative stress | thermotolerance | genetically modified organism | biofuel | hydroxyl radical

Agroforestry tree plantations have been increasing globally and are used for diverse purposes, including the production of wood and food products, the establishment of wind breaks and biofiltration facilities, and most recently as a feedstock for biofuel production (1–3). The high biomass production rates that can be achieved with fast-growing tree varieties (especially for poplars, eucalypts, and palms) are often accompanied by high rates of leaf isoprene emission. Isoprene produced during light-dependent metabolism in the chloroplasts of many tree species, especially those with high productivity rates, is volatile and is emitted globally at rates that are similar to methane emissions (4). Unlike methane, however, emitted isoprene is photochemically oxidized within hours, not years. Through a series of chemical reactions, the atmospheric oxidation of isoprene enhances the production of oxidative pollutants, such as tropospheric ozone (O_3) and organic nitrates (e.g., PAN) in urban and suburban areas; increases the global lifetime of the radiatively active, trace-gas methane (CH_4); and promotes the growth of secondary organic aerosol (SOA) particles, which affect the short-wave radiation budget of Earth (5–8). Using a coupled Earth-system and chemistry model, it has been shown that expansion of poplar plantations in Europe to meet 2020 biofuel targets will potentially increase premature human deaths up to 6% and reduce the yield of wheat and maize crops by 9 $Mt \cdot y^{-1}$ because of increased isoprene emission and accompanying O_3 production (9, 10). In Southeast Asia, isoprene-emitting oil-palm plantations increased in total production by a factor of 5 between 1994–2014 as part of an effort to increase food oil and biofuels (11), causing an increase in near-surface O_3 concentration of 3.5 to 15 ppbv (12, 13).

The genetic modification of agroforest trees to minimize leaf isoprene emission is feasible (14). However, these efforts have been largely dismissed in the past with assumptions that the trait

Significance

Leaf isoprene emission, a trait that promotes tree stress tolerance but also affects air quality and climate, has been genetically suppressed in hybrid-poplar cultivars without influencing plantation biomass production in 2 field trials. Induction of compensatory increases in protective proteomic components and a phenological growth pattern that favors most biomass production during less stressful parts of the growing season likely explain the apparent paradox of high plantation production with low isoprene emission. We show that it is feasible to develop sustainable plantation-scale biomass sources that can serve as fossil-fuel alternatives for energy generation and lignocellulosic resource development, without degrading air quality.

Author contributions: R.K.M., B.W., T.N.R., S.H.S., D.J.P.M., J.B., and J.-P.S. designed research; R.K.M., B.W., T.N.R., K.B., J.M..-P., S.H.S., K.A., J.M., D.J.P.M., N.A.T., A.A.N., I.S., G.A.B.-G., P.I., J.T.M., J.B., and J.-P.S. performed research; R.K.M., B.W., T.N.R., K.B., J.M..-P., S.H.S., K.A., J.M., D.J.P.M., N.A.T., A.A.N., I.S., G.A.B.-G., P.I., J.T.M., J.B., and J.-P.S. analyzed data; and R.K.M., B.W., T.N.R., S.H.S., D.J.P.M., and J.-P.S. wrote the paper.

The authors declare no competing interest.

This article is a PNAS Direct Submission. A.K.-S. is a guest editor invited by the Editorial Board.

Published under the PNAS license.

Data deposition: The mass spectrometry proteomics data have been deposited in the ProteomeXchange Consortium at http://proteomecentral.proteomexchange.org/cgi/GetDataset using the dataset identifier PXD013252. All other data created for this study have been deposited in the Open Science Framework data repository and are accessible at the unique identifier https://osf.io/xzndc/?view_only=b3233c6ab9384e189a56282ef7c0e5fe.

[1]To whom correspondence may be addressed. Email: russmonson@email.arizona.edu, rosensti@pdx.edu, or jp.schnitzler@helmholtz-muenchen.de.

This article contains supporting information online at https://www.pnas.org/lookup/suppl/doi:10.1073/pnas.1912327117/-/DCSupplemental.

Downloaded at UNIVERSITY OF ARIZONA on January 8, 2020

1) is advantageous for the tolerance of abiotic stresses, such as those due to high temperature, low atmospheric humidity, and acute drought (15, 16), and 2) correlates positively with photosynthetic CO_2 assimilation (17). Removal of the trait has been predicted to result in reduced productivity and declines in plant fitness, especially in the face of future climate change (18–20). Studies of genetically modified poplars grown in controlled-environment growth conditions, however, indicate that stress interactions are complex. Several studies have shown that although isoprene emission protects trees from abiotic stress, increases in atmospheric CO_2 concentration cause a decrease in isoprene biosynthesis, thus reducing that protection (21–23). Increases in global temperatures, however, have the potential to mitigate the elevated CO_2 effect (24, 25), increasing the protective effect of isoprene emissions, even in the presence of elevated CO_2 (26). In the case of drought, non–isoprene-emitting tobacco plants that have been genetically transformed to produce isoprene exhibited a reduction in biomass production during drought, compared to wild-type plants, suggesting a growth cost to the stress protection normally provided by isoprene (27). While it is difficult to generalize about the role of isoprene emissions as a necessary stress-tolerance trait and its cost to biomass production in the face of future global change, most analyses indicate that isoprene emissions from global forests are indeed likely to increase in the future (28).

The cellular mechanisms that enhance stress tolerance and photosynthetic performance due to isoprene emission have not been resolved. Past theories of direct stabilization of chloroplast membranes through the hydrophobic solubilization of isoprene have not been supported (29, 30). More recent theories focus on a cellular signaling role that involves modulation of several stress-related gene networks (31, 32). There is a need to continue assessing the roles and mechanisms of isoprene protection against abiotic stresses in a broader set of environmental settings and with the synergistic challenges from interacting stresses, such as those that occur under natural field conditions.

In this study, we used gene silencing through RNA interference (RNAi) to reduce leaf isoprene emission to negligible levels in several genetic lines (independent gene insertions) of hybrid poplar, which were grown in multiple-year field trials at 2 geographically distinct plantation sites, where we evaluated stress tolerance, remodeling of cellular metabolism, photosynthetic function, and woody biomass production. One site was located near Corvallis, OR, and was intended as an analog to commercial poplar plantations that are located in the Pacific Northwest of the United States. For example, the largest commercial poplar plantation in North America (10,118 ha and 7.5 million trees) was in operation for over 20 y (1992 to 2017) near Boardman, OR, located 312 km NE from our experimental plantation near Corvallis. The second site was located near Tucson, AZ, and was intended to test whether biomass production is compromised by elimination of isoprene emission in one of the hottest and least humid climates in North America. We tested the hypothesis that isoprene biosynthesis and emission are required traits for high rates of aboveground woody biomass production in the agroforestry plantation environment.

Results

Eighteen genetically modified poplar lines and one wild-type control (CN) were grown for 3 y in the Oregon plantation (*SI Appendix*, Fig. S1). Three of the modified lines were isoprene-emitting empty-vector (EV) controls and 15 lines were modified for suppressed isoprene emissions. For clarity, we refer to the 3 EV lines and 1 CN line, together, as isoprene-emitting (IE) genotypes and the 15 low-isoprene emitters as isoprene-reduced (IR) genotypes. Reductions in isoprene emission were nearly complete in some IR lines and only slightly reduced in others, based on statistical metrics provided by analysis of variance (ANOVA for genotype effect on isoprene emission rate: $F = 56.978$, degrees of freedom [df] = 12, $P < 0.001$; Fig. 1 *A* and *C*). The reduction in leaf isoprene emission did not result in reduced rates of photosynthesis (ANOVA for genotype effect on photosynthesis: $F = 0.90$, df = 8, $P = 0.52$; Fig. 1 *B* and *D*) or woody aboveground biomass production (Fig. 2) (ANOVA for genotype effect on biomass, $F = 1.075$, df = 18, $P = 0.375$; ANOVA for year effect on biomass, $F = 33.259$, df = 1, $P < 0.001$; ANOVA for genotype × year effect on biomass, $F = 0.872$, df = 18, $P = 0.6138$). For example, in the Oregon plantation, biomass production in lines IR-70 and IR-88, which exhibited negligible rates of isoprene emission, had photosynthesis rates (Fig. 1*B*)

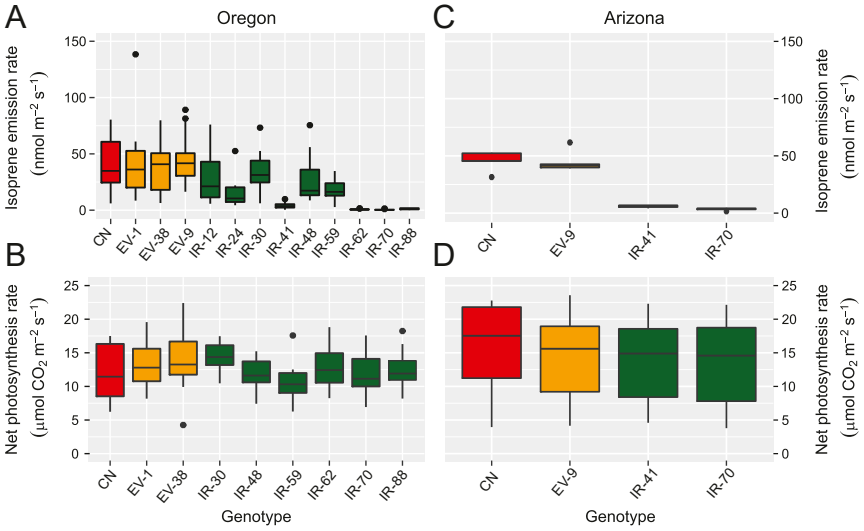

Fig. 1. (*A*) Maximum observed leaf isoprene emission rates in 13 hybrid poplar genetic lines growing in Oregon. Horizontal lines within each box represent median values; boxes represent the limits of the second (lower) and third (upper) quartiles, respectively; vertical lines represent upper and lower ranges; and dots represent extreme outliers (n = 5 trees for each line). (*B*) Maximum observed leaf net photosynthesis rates in 9 of the 13 genetic lines growing in Oregon. (*C*) Maximum observed leaf isoprene emission rates in 4 hybrid poplar genetic lines growing in Arizona. (*D*) Maximum observed leaf net photosynthesis rates in the 4 genetic lines growing in Arizona. In all cases, n = 5 trees. All measurements were made on separate trees for each genetic type and plantation.

Downloaded at UNIVERSITY OF ARIZONA on January 8, 2020

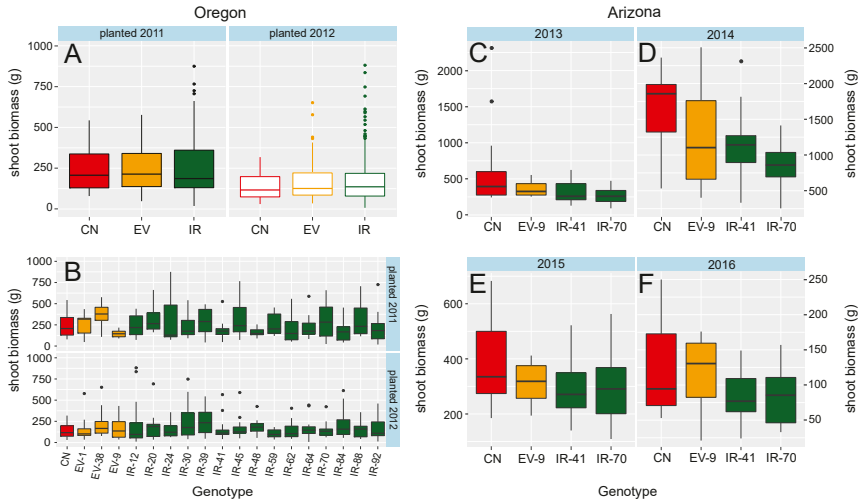

Fig. 2. (*A*) Summary of total harvestable shoot biomass for binned genetic lines of trees grown in Oregon in 2011 and 2012 and harvested spring 2015. Boxes, whiskers, and symbols are as described in Fig. 1. (*B*) Summary of total harvestable shoot biomass for individual genetic lines grown in Oregon in 2011 and 2012 and harvested spring 2015. (*C–F*) Annual shoot biomass production in 4 consecutive years for the 4 genetic lines grown in Arizona. For all cases, n = 12 trees for each genotype and plantation.

and aboveground biomass production rates (Fig. 2*B*) that were not substantially different from those of the 4 IE lines. Eight genetic lines representing IE and IR trees from the Oregon plantation were excavated in spring 2015, after 3 y of growth, for sampling of cumulative belowground biomass. Belowground production did not differ systematically among the IR and IE lines (ANOVA for genotype effect [biomass log transformed]: F = 1.9832, df = 7, P = 0.0652; *SI Appendix*, Fig. S2).

Four of the genetic lines (CN, EV-9, IR-41, and IR-70) were grown for 4 y in an experimental plantation near Tucson, AZ (*SI Appendix*, Fig. S1). Maximum daily air temperatures during the 4 warmest months of the summer (June, July, August, and September) averaged 35.6 ± 2.1 (SD) °C across the 4 y (2013 to 2016) of experimental observation. Twelve trees from each genetic line were exposed to high fertilization and irrigation rates during 2012 and 2013 and reduced or eliminated fertilization and irrigation during 2014 and 2015. With this experimental design we aimed to examine biomass production under conditions of both high (well-fertilized, well-watered) and low (light fertilization, limited-watering) growth potentials. Continuous monitoring of canopy temperatures throughout most of the growing season in 2014 revealed that maximum daily leaf temperature exceeded 32 °C on most days and was ∼40 °C on many days (*SI Appendix*, Fig. S3 *A–C*). Direct observations of individual leaf temperatures with thermocouples attached to the underside of leaves during midsummer in 2014 confirmed that even with replete irrigation and high transpiration rates, leaf temperatures were within 6 to 7 °C of maximum midday air temperatures and spent much of the midday period above 35 °C (*SI Appendix*, Fig. S3*D*).

In the Arizona plantation, when considering the 3 lines influenced by RNAi treatments—the empty-vector IE control and 2 IR lines—we observed no significant differences in annual aboveground biomass production during or following 4 y of growth (Fig. 2; ANOVA for genotype effect on biomass, F = 1.2575, df = 2, P = 0.2878; see *SI Appendix*, sections S2 and S3 for details of the ANOVA analysis). There were, however, some effects of genotype and year on specific patterns of biomass increase. The elevated levels of fertilization and irrigation during the first 2 y of growth culminated in higher production in all lines during the second year of the experiment, compared to all other years (ANOVA for genotype effects on biomass: F = 109, df = 12 blocks, P < 0.05). The only clear effect of genotype on aboveground biomass in the Arizona plantation was caused by the wild-type CN line growing ∼85% more than the other lines in year 2 (ANOVA for all 4 genotypes, 2014: F = 4.9, df = 12 blocks, P = 0.05) (Fig. 2*D*). Even during this year, however, we observed no significant differences in woody biomass production between the empty-vector (EV-9) line, which emits isoprene at the same rate as the CN line, and the 2 IR lines (ANOVA for 3 selected genotypes: F = 1.2, df = 12 blocks, P = 0.28). Thus, the lower growth rates exhibited by the modified lines do not appear to be due to the emission of isoprene, but rather to the genetic modification process. In years 3 (2015) and 4 (2016), when fertilizer and irrigation were reduced, there were no differences in production between the IE and IR lines in the Arizona plantation. We concluded that overall the presence of isoprene emission had no effect on biomass increase during all 4 y in the Arizona plantation, but that genetic manipulation, independent of effects on isoprene emission, impaired biomass production in the 3 genetically modified lines (EV and 2 IR lines), compared to the wild-type CN line, when grown in the high-resource conditions presented in year 2.

A subset of 5 plants from each of the 4 genetic lines in the Arizona plantation was selected for root excavation at the end of year 4. There was a trend toward lower mean belowground biomasses in the IR lines, compared to the IE lines (*SI Appendix*, Fig. S2), but the trend could not be justified as statistically significant (F = 4.234, df = 1, P = 0.056). Furthermore, when considering all 4 lines together, an effect of genotype was not observed (F= 1.525, df= 3, P = 0.246). Due to the statistical weakness of the observation of slightly lower belowground biomass in the IR lines, we have not taken this result to a deeper level of interpretation. However, it may indicate that not all poplar lines are equally suitable for genetic modification aimed at maximizing production. If so, more work is justified to determine whether this variation could be used as a criterion for future genotype selection.

Seasonal growth of aboveground biomass began in early April at the Arizona plantation and biweekly observations showed rapid increases in stem-diameter increment until the middle of May (*SI Appendix*, Fig. S4). The early-season rapid growth phase occurred while maximum daily temperatures fluctuated between 20 and 31 °C. During the hottest and driest part of the growing season, when maximum canopy temperatures were 35 to 40 °C, diameter growth of all branches in the 4 lines slowed from an

Downloaded at UNIVERSITY OF ARIZONA on January 8, 2020

average of 2 mm·d^{-1} prior to May 20 to 0.3 mm·d^{-1} after May 20. There were no significant differences in growth between the IE and IR lines at any date during the growing season.

Leaf net photosynthesis rates in the Arizona trees decreased at temperatures above 25 °C (Fig. 3). Rates of photosynthesis were slightly lower in the EV and IR lines, compared to the wild-type CN line, during the June sampling campaign, when seasonal temperatures were at a maximum. However, the net assimilation rates were not significantly different between the EV and IR lines, despite high isoprene emissions from the EV line. Thus, when all 4 lines, together, were analyzed for an effect of isoprene emission on photosynthesis rate, there was no significant difference (ANOVA for effect of genotype on photosynthesis at 27 °C: $F = 0.2519$, $df = 3$, $P = 0.86$). During April, when ambient temperatures were still relatively cool, and late September, when canopy temperatures persisted above 30 °C, there was also no evidence of improved photosynthetic performance in the IE lines, compared to the IR lines. Leaf concentrations of total flavonoids and a leaf-nitrogen index were significantly different between IE and IR lines when sampled at the end of the warmest parts of the growing season (*SI Appendix*, Fig. S5 and section S6). No significant differences between IE and IR trees were observed for leaf anthocyanin or chlorophyll content in all field conditions (*SI Appendix*, section S6).

We conducted analyses of the leaf proteome to study the overall scope of genetic modification that occurred, either directly or indirectly, as a result of isoprene suppression. Proteomic analysis provides insight into the protein composition of the leaf at a point in time, which in turn reflects the biochemical and functional conditions within which plant metabolism takes place. Unlike genomic analyses, which reflect long-term generational changes in gene composition, or metabolomic analyses, which reflect short-term (milliseconds-to-minutes) changes in metabolic substrates and products, proteomic analyses provide insight into changes in overall metabolic potential due to gene expression (at a timescale of seconds to hours). Analysis of the proteome in leaves from the Arizona plantation at predawn and noon in June 2013 (the first year of the growth analysis), when temperatures were at a seasonal maximum, revealed numerous differences among the IE and IR lines (Table 1 and Fig. 4). Proteomic profiles of the IE and IR lines were distinguished by the orthogonal partial least-squares (OPLS) method with 10% explained variance (Fig. 4*A*). In total we identified 169 discriminant proteins—113 lower expressed and 56 higher expressed—in the IR lines, compared to IE lines (Fig. 4 *B* and *C*). Principal component analysis revealed that both suppression of isoprene emission (operating at the scale of ontogeny) and time of day (operating at the scale of diurnal environmental variation) operated as primary controls over proteome expression patterns. Most of the expression differences between the IR and IE lines were found during predawn sampling—38 proteins were exclusively up-regulated and 88 proteins were exclusively down-regulated at predawn, compared to 8 exclusively up-regulated and 10 exclusively down-regulated at noon (Fig. 4 *D* and *E*). A total of 10 proteins were up-regulated and 15 were down-regulated in both the predawn and noon samples. The 10 most regulated proteins for predawn samples and noon samples, respectively, are presented in Table 1. Two of the most repressed proteins (negative $\log_2$-fold IR/IE change) were associated with isoprene synthase (Potri.007G118400.1 and Potri.017G041700.1), confirming the effective nature of the RNAi treatments in causing suppression of this enzyme. Significant ($P \leq 0.05$ between IR and IE lines) down-regulation in the absence of isoprene emissions occurred for proteins involved in the phenylpropanoid pathway and flavonoid biosynthesis. Significant up-regulation occurred for several proteins involved in the biosynthesis of terpenoids and carotenoids and one protein involved in the biosynthesis of α-tocopherol (vitamin E). Some proteins involved in the methylerithritol phosphate (MEP) and jasmonic acid pathways were also among those exhibiting increases in expression in the face of isoprene suppression. A complete list of proteomic changes is provided in *SI Appendix*, Table S1.

A Voronoi Treemap analysis provided pathway-wide patterns of proteomic rearrangements (Fig. 5 *A* and *B*). In the case of flavonoid biosynthesis, the entire pathway was consistently and highly down-regulated in the IR trees. The phenylpropanoid pathway, which supplies flavonoid biosynthesis with substrate, was differentially regulated. Phenylalanine ammonia-lyase (PAL), the first enzyme in the pathway, was down-regulated in IR trees, similar to the pattern for flavonoid biosynthesis, but cinnamyl-alcohol dehydrogenase (CAD) content, one of the last enzymes in the pathway, was up-regulated. Interestingly, CAD represents the first step toward commitment to lignin biosynthesis. Thus, suppression of isoprene emissions may cause a shift away from flavonoid biosynthesis and toward lignin biosynthesis, favoring woody biomass production. In the case of terpenoid biosynthesis,

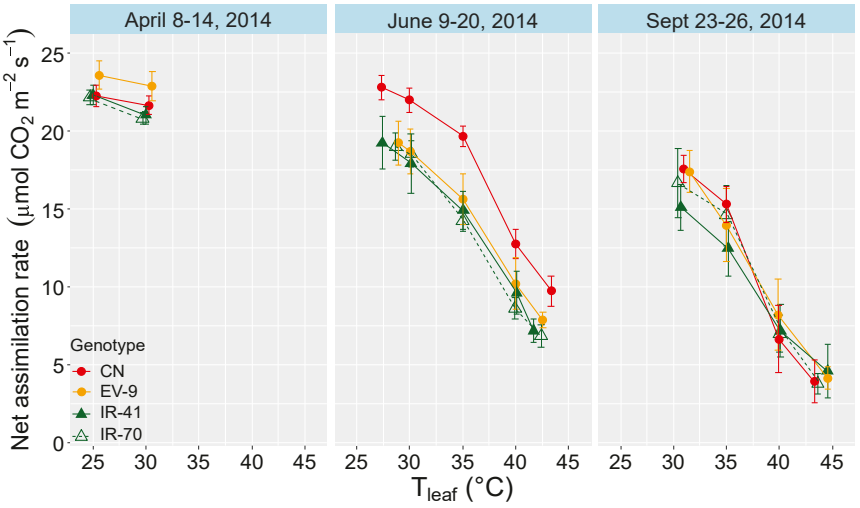

Fig. 3. Rates of net photosynthetic carbon assimilation as a function of leaf temperature observed at 3 times during the growing season for the 4 genetic lines of poplar grown at the Arizona plantation. Points represent the mean (n = 5 separate trees) and vertical bars represent ±SE.

Downloaded at UNIVERSITY OF ARIZONA on January 8, 2020

Table 1. A list of the 10 most down-regulated (ranked by log_2-fold change IR/IE <0) and up-regulated (log_2-fold change IR/IE >0) proteins at predawn and noon

Potri ID	Log 2, IR/IE	−Log 10, P_{adj}	Pathway	Enzyme/protein
Predawn				
Down-regulated				
007G118400.1	−3.372	8.29	Isoprene biosynthesis	Isoprene synthase (ISPS)
017G041700.1	−3.241	11.04	Isoprene biosynthesis	Isoprene synthase (ISPS)
009G133300.1	−1.975	1.56	Anthocyanin biosynthesis	Anthocyanidin 3-O-glycosyltransferase
001G051600.1	−1.694	2.63	Flavonoid biosynthesis	Naringenin-chalcone synthase (CHS)
007G018900.1	−1.461	5.21	Fatty-acid biosynthesis	Soluble epoxide hydrolase (SEH)
013G022100.1	−1.342	2.31	9-Lipoxygenase pathway	Linoleate 9S-lipoxygenase
014G145100.1	−1.188	2.96	Flavonoid biosynthesis	Naringenin-chalcone synthase (CHS)
005G229500.1	−1.119	1.44	Leucocyanidin biosynthesis	Dihydrokaempherol 4-reductase
005G162800.1	−1.079	1.80	Chorismate biosynthesis	3-deoxy-7-phosphoheptulonate synthase
003G173000.1	−1.010	2.71	Aerobic respiration	Ubiquinone reductase
Up-regulated				
016G066100.1	1.966	2.00	Sucrose biosynthesis	Sucrose-phosphate phosphatase (SPP)
005G025700.1	1.928	3.56	Terpenoid biosynthesis	Rubber elongation factor protein (REF)
001G055300.1	1.201	3.00	Terpenoid biosynthesis	Rubber elongation factor protein (REF)
004G135300.1	1.099	1.54	Betalamic acid biosynthesis	Stizolobate synthase
004G140800.1	1.080	1.45	Nitrate reduction	Ferredoxin-nitrite reductase
002G081800.1	0.952	3.19	Ethanol degradation	Aldehyde dehydrogenase (NAD^+)
018G088600.1	0.812	1.62	Triacylglycerol degradation	Triacylglycerol lipase
014G148700.1	0.776	3.56	Lycopene biosynthesis	9,9′-dicis-zeta-carotene desaturase (ZDS)
007G044300.1	0.708	3.38	Carotenoid biosynthesis	Zea-epoxidase (ZEP)
009G111600.1	0.598	4.89	Methylerythritol phosphate pathway	4-Hydroxy-3-methylbut-2-enyl diphosphate (ispH)
Midday				
Down-regulated				
017G041700.1	−3.655	10.86	Isoprene biosynthesis	Isoprene synthase (ISPS)
007G018900.1	−2.241	7.66	Fatty acid biosynthesis	Soluble epoxide hydrolase (sEH)
001G449500.1	−0.710	4.18	Starch biosynthesis	Glucose-starch glucosyltransferase (WAXY)
004G139700.1	−0.922	4.05	Flavonoid biosynthesis	Flavanone 3-dioxygenase (F3H)
007G118400.1	−3.039	3.94	Isoprene biosynthesis	Isoprene synthase (ISPS)
016G091100.1	−0.816	2.85	Phenylpropanoid biosynthesis	Phenylalanine ammonia-lyase (PAL)
019G130700.1	−0.720	2.01	Phenylpropanoid biosynthesis	Transcinnamate 4-monooxygenase
016G057400.1	−0.508	1.99	Starch/sucrose metabolism	Glucan endo-1,3-beta-D-glucosidase
001G462800.1	−0.817	1.75	Alkaloid biosynthesis	Tetrahydroberine oxidase
008G038200.1	−1.058	1.73	Phenylpropanoid biosynthesis	Phenylalanine ammonia-lyase (PAL)
Up-regulated				
005G025700.1	1.694	6.15	Terpenoid biosynthesis	Rubber elongation factor protein (REF)
001G055300.1	1.044	3.49	Terpenoid biosynthesis	Rubber elongation factor protein (REF)
004G102000.1	0.702	3.48	Jasmonic acid biosynthesis	4-Coumarate-CoA-ligase (4CL)
007G044300.1	0.506	3.08	Carotenoid biosynthesis	Zea-epoxidase (ZEP)
002G081800.1	0.795	2.94	Ethanol degradation	Aldehyde dehydrogenase (NAD^+)
014G148700.1	0.526	2.85	Lycopene biosynthesis	9,9′-dicis-zeta-carotene desaturase (ZES)
011G099400.1	0.668	2.76	Terpenoid biosynthesis	11-Oxo-β-amarin 30-oxidase
018G088600.1	1.021	2.41	Triacylglycerol degradation	Triacylglycerol lipase
002G018300.1	2.087	1.87	Phenylpropanoid biosynthesis	Cinnamyl-alcohol dehydrogenase (CAD)
018G040200.1	0.594	1.72	Vitamin E (tocopherol) biosynthesis	(delta-)tocopherol cyclase

Only those proteins with confirmed annotations are included. Protein abbreviations refer to those shown in Fig. 4. See *SI Appendix*, Table S1 for full list of regulated proteins. Bold-type designations in the first column refer to proteins involved in constitutive (noninduced) metabolism.

enzymes were consistently and highly up-regulated across each associated pathway in the IR trees. For the MEP pathway, which provides precursors to terpenoid biosynthesis, protein expression was moderately and consistently increased (or in the case of one protein, unchanged) in the IR trees. These patterns indicate a shift in the IR trees away from the synthesis of volatile isoprene and toward the synthesis of higher terpenoids (i.e., lutein and β-carotene). In the jasmonic acid pathway, changes in protein expression were mixed, with some proteins increasing and some decreasing. The fact that the proteomic rearrangements that we observed were evident during the first year of growth indicates a relatively quick response to the genomic and environmental conditions of the genetically modified trees.

Discussion

Our study has revealed that it is possible to genetically modify agroforestry poplar trees to reduce plantation isoprene emissions, without compromising woody biomass production. Several past studies have shown that suppression of isoprene emissions is correlated with reduced tolerance of high temperature (33, 34) and oxidative stress (35, 36) in isolated leaves; leaf temperatures as low as 30 °C and moderate levels of water stress have been shown to inhibit photosynthetic performance in the absence of isoprene emission (37, 38). These observations have led to a general hypothesis that isoprene emissions protect leaves, even under relatively modest levels of abiotic stress (39, 40). The conclusions from our study show that when trees are grown in

Downloaded at UNIVERSITY OF ARIZONA on January 8, 2020

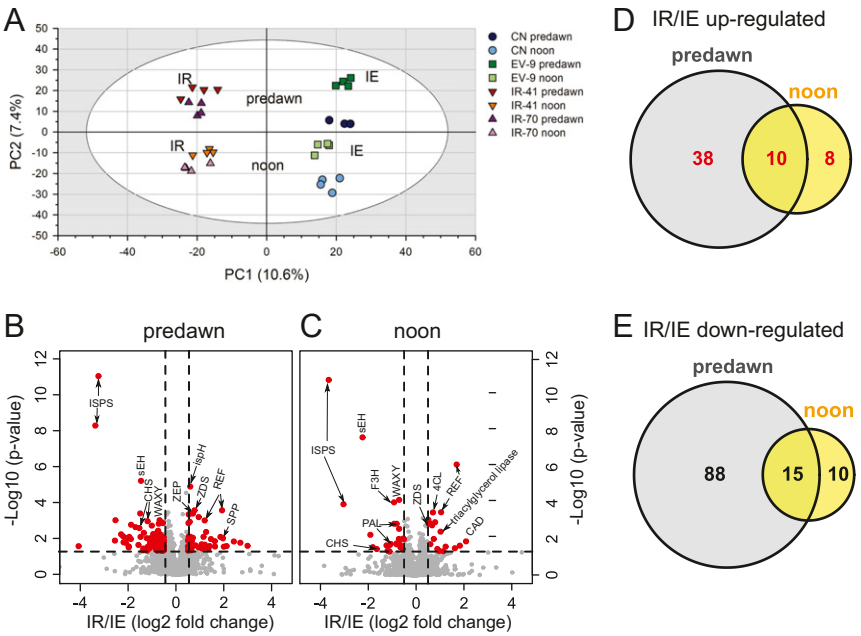

Fig. 4. Whole-proteome comparison of IE and IR leaves sampled during predawn and midday (noon) for trees grown in Arizona. (*A*) Score plot of OPLS modeling showing distribution of principal components. Samples were categorized as IE and IR and according to the respective sampling time (predawn, noon). The ellipse indicates the tolerance of the analysis based on Hotelling's T^2 with $P = 0.05$. (*B* and *C*) Volcano plots showing the magnitude of differential protein abundance in IR and IE genotypes (log_2 fold change) compared with the measure of statistical significance ($-log_{10}$ [P value, beta binominal test]). Vertical dashed lines indicate a log_2-fold change of ±0.5 and the dashed horizontal line indicates the significance level of $P \leq 0.05$. Proteins that fit both criteria are shown as red dots. Exemplary proteins with the highest significance and log_2-fold change, respectively, are specifically identified by abbreviations (see Table 1 for complete protein names) according to Ptrichocarpa_210_v3.0_defline. The relative differences between IR and IE lines are indicated on the x axis as a ratio (IR/IE) in the positive or negative direction. (*D* and *E*) Venn plots indicating the number of significantly ($P \leq 0.05$) up-regulated (*D*, log_2-fold change IR/IE >0) and down-regulated (*E*, log_2-fold change IR/IE <0) proteins at predawn and noon, as well as constitutive proteins, i.e., observed at both sampling events.

poplar plantations under natural field conditions, any physiological benefit of isoprene emission with regard to stress tolerance and aboveground productivity is either not relevant or subject to compensation by alternative protective pathways following RNAi suppression and subsequent proteomic and metabolomic adjustments (20).

There is evidence in our observations that, when considered alone, might predict reductions in plantation productivity in the face of suppressed isoprene emissions, the opposite of what we observed. For example, in early June, when maximum canopy temperatures were often greater than 40 °C (*SI Appendix*, Fig. S3), net photosynthesis rates were significantly suppressed in the 2 IR lines, compared to the isoprene-emitting CN line (Fig. 3). These results might be used to conclude that suppression of isoprene emission resulted in decreased photosynthetic performance in the IR trees during the hottest part of the growing season. However, there were no significant differences between the 2 IR lines and the EV line, which serves as the true control to the RNAi lines and also emits isoprene at natural levels. Thus, the photosynthetic temperature-response curves shown in Fig. 3 do not, in fact, accurately predict performance of trees, due to lack of isoprene emission, in the plantation environment.

Separately, we observed that flavonol and anthocyanin compounds were reduced more in the IR lines than in the IE empty-vector control (EV-9), in the Arizona plantation. Suppression of flavonol and anthocyanin synthesis has been observed in these same IR lines in past studies of greenhouse- and chamber-grown trees (20, 41). These compounds have been shown to provide greater tolerance of drought stress in poplar trees (42), and they reduce the load of photochemically generated oxidative compounds, such as H_2O_2, during heat stress (20). Furthermore, exogenous fumigation of the isoprene nonemitting species *Arapidopsis thaliana* with isoprene (43) and genetic transformation of the isoprene nonemitting species *A. thaliana* and *Nicotiana tabacum*, to emit isoprene (32, 44), caused an increase in expression of the pathways that produce flavonols and anthocyanins and increased drought resistance in the case of *N. tabacum* (44). Thus, there are reasons to predict that reductions in flavonol and anthocyanin synthesis in the IR trees from our studies should have negatively influenced their tolerance of high temperatures and drought. Given this, it is of interest that we could not find consistent evidence of a negative influence of high seasonal temperatures and low atmospheric humidities during all 4 y, and imposed drought during year 4, on the growth of IR trees in the Arizona and Oregon plantations.

We offer 2 explanations for the lack of an observed isoprene effect on photosynthetic function and biomass production in the natural plantation environment. Together, the explanations provide room for the coexistence of past findings of a positive role of isoprene emission in facilitating abiotic stress tolerance and our observations of no influence on observed biomass accumulation. First, most of the woody biomass was produced during the early part of the growing season, prior to the midsummer occurrence of extremely hot and dry weather. The phenological context of tree growth in midlatitude, Northern Hemisphere forests has seldom been considered in past discussions of the physiological benefit of isoprene emission. Most studies have focused on isolated, fully expanded leaves observed during an artificially imposed, acute stress. The preponderance of this type of study in the isoprene-emission literature has largely shaped current views about how this trait provides its greatest adaptive potential. The assumption that plant persistence and fitness are improved through greater tolerance of acute abiotic stress during that portion of the growing season

Downloaded at UNIVERSITY OF ARIZONA on January 8, 2020

that is least favorable for growth is embedded in a larger assumption that isoprene emission enhances survivability, not productivity. Thus, even considering the extensive past literature, it is not necessarily expected that removal of the trait will result in reduced productivity and fitness, especially during the less stressful periods during the growing season. Our research is consistent with this view—that loss of the trait will have less, or no, impact on biomass production during the most productive portion of the growing season, but may enhance fitness during extreme climate events. Placing isoprene emissions within a proper adaptive context will sharpen our ability to understand how forest communities and landscapes will respond to future climate shifts, which are expected to increase the frequency of anomalously hot and dry weather episodes.

With regard to the second explanation, past studies have shown that suppression of isoprene emission by RNAi transformation in these same poplar lines results in remodeling of the chloroplast proteome and metabolome in a way that increases the scavenging of reactive oxygen species (ROS) and thus minimizes the oxidative damage expected from suppression of isoprene biosynthesis (45, 46). Thus, while several past studies have shown that isoprene acts as a positive signal that enhances stress tolerance (32, 43, 44), the studies by Velikova et al. (45) and Ghirardo et al. (46) showed that the suppression of isoprene emission can also cause compensatory increases in pathways, such as those for the terpenoids lutein and β-carotene, that take over some of isoprene's protective capacity. In our study, we observed similar proteomic changes that could compensate for the loss of isoprene biosynthesis and thus protect the trees from abiotic stress due to high leaf temperatures and low atmospheric humidity. We observed an overall and consistent up-regulation of proteins in the pathways that control terpenoid, carotenoid, and α-tocopherol biosynthesis in the IR trees (Table 1 and Fig. 4). The up-regulated expression of components in these pathways may take on oxidative protection functions similar to those of flavonols and anthocyanins, which are suppressed, along with the phenylpropanoid pathway, in the absence of isoprene signaling. Our results contribute to a paradigm shift that is occurring in the community of researchers considering isoprene-stress relations (20, 31, 44). Whereas past research provided evidence of a direct role of isoprene in protecting photosynthetic membranes and protein complexes from oxidative attack, more recent research is pointing to an additional and potentially more important role of isoprene as a cellular signaling molecule. In this new hypothesis, isoprene takes on the role to control the expression of pathways that potentially compete for chloroplast substrates and produce multiple compounds with roles in protection from climate stress, oxidative stress, herbivore stress, and the multiple interactions of these stresses with intrinsic plant growth regulators. In the absence of isoprene emissions, the phenylpropanoid pathway is suppressed and the isoprenoid pathways that produce complex terpenoids and carotenoids are enhanced (for flux rates, see ref. 46). The compensatory expression of these pathways in the IE and IR trees may explain the lack of our observed response of tree growth to the suppression of isoprene emissions. Clearly, the interactions of multiple pathways under the influence of isoprene signaling are complex. Our work sets the stage for further research into the potential for trait tradeoffs in the area of isoprene emission, stress tolerance, and plant growth. The changes in protein expression, and the new chemical products that they produce, if incorporated into new lines of cultivated poplar, will likely have several higher-order influences on the global environment and human health, including the potential for new modes of influencing atmospheric photochemistry (depending on the nature and amount of terpenoid biosynthesis) and associated effects on agricultural production and human respiratory health.

Planted poplar plantations used for woody biomass production currently occupy ∼9.4 million ha, globally, an area which has increased from ∼3.9 million ha since 2004 (47, 48). The impacts of continued climate change and the expansion of plantation forests are predicted to cause significant increases in regional and global biogenic isoprene emissions (28, 49). Isoprene emissions from forests have been linked to several photochemical processes that alter the oxidative capacity of the lower atmosphere and increase the burden of atmospheric greenhouse gases, such as methane and ozone (7). The heterogeneous condensation of oxidized derivatives of isoprene causes increased growth rates in secondary organic aerosols in the atmosphere, which affect Earth's radiative balance (50, 51). Our study represents a field trial of genetically modified poplar trees with negligible rates of isoprene emission. If future efforts are successful in reducing forest plantation isoprene emissions, we can expect multiple opposing and complex influences on positive and negative climate forcings. In the lower atmosphere, isoprene exerts several influences on climate-relevant processes: 1) It amplifies rates of O_3 production in nitrogen oxide (NO_x)-rich urban and suburban areas, 2) it promotes rates of O_3 destruction in low-NO_x rural and remote areas, 3) it catalyzes hydroxyl-radical recycling pathways which affect the atmospheric lifetime of CH_4, and 4) it is oxidized to multiple products that contribute to the growth of SOA particles. The size distribution and density of SOA particles affect not only Earth-surface climate, but also the distribution of direct and diffuse photosynthetically active photon fluxes within the canopy environments of forests, further complicating evaluations of projected global gross primary productivity and its relationship to isoprene emissions from native forests. Recent efforts have been initiated to evaluate the integrated effects of these atmospheric influences (52), and it is this type of complex photochemical modeling that is most likely to provide comprehensive predictions of how future changes in plantation isoprene emissions might influence global climate.

Decisions concerning regional land use are also likely to influence global plantation isoprene emissions and associated climate effects. A recent analysis of global shifts in forest coverage showed a small influence on isoprene emissions during the period 2000 to 2015 (1.5% decrease), although specific regional influences, such as in the tropics, were greater (53). Future patterns of land-use change, particularly those involving replacement of native forests with cultivated plantations, are likely to cause increases in isoprene emission, concomitant with increases in tropospheric O_3 production and SOA particle growth (28). Our research provides an alternative perspective on these potential outcomes. The fact that cultivars of poplar can be produced in a way that reduces isoprene emission while preserving high rates of biomass production provides optimism toward achieving greater environmental sustainability while expanding sources for fossil-fuel alternatives and lignocellulosic resources. We anticipate several challenges as the findings of our studies are transferred into forestry practice. First, expanded research is needed to establish whether our results apply to the diversity of genotypes, species, and environments in which commercial trees are grown. Second, it is desirable that both conventional and recombinant DNA approaches to genetic manipulation are explored given the existence of regulatory and market constraints to the use of genetic engineering for commercial applications (54). Interestingly, CRISPR gene editing may be a more efficient means for isoprene reduction than the RNAi method that we studied and may be exempt from regulation in the United States and several other countries—making it easier to employ (55).

Methods

Genetic Modification of Poplar Lines. The down-regulation of isoprene emission by RNA interference in gray poplar (*Populus* x *canescens*) was performed with the same poplar (no. 7171-B4, Institute de la Recherche Agronomique

Downloaded at UNIVERSITY OF ARIZONA on January 8, 2020

[INRA], Nancy, France) and *Agrobacterium tumefaciens* (C58C1/pMP90) strains as described earlier (18). Sense and antisense gene fragments of a 160-bp isoprene synthase-specific gene segment of the transit peptide sequence (position 21 to 181) were cloned as a self-complementary hairpin construct into the pKANNIBAL vector, followed by transfer into the binary vector pART27. The RNAi cassette and the empty pART27 vector were then

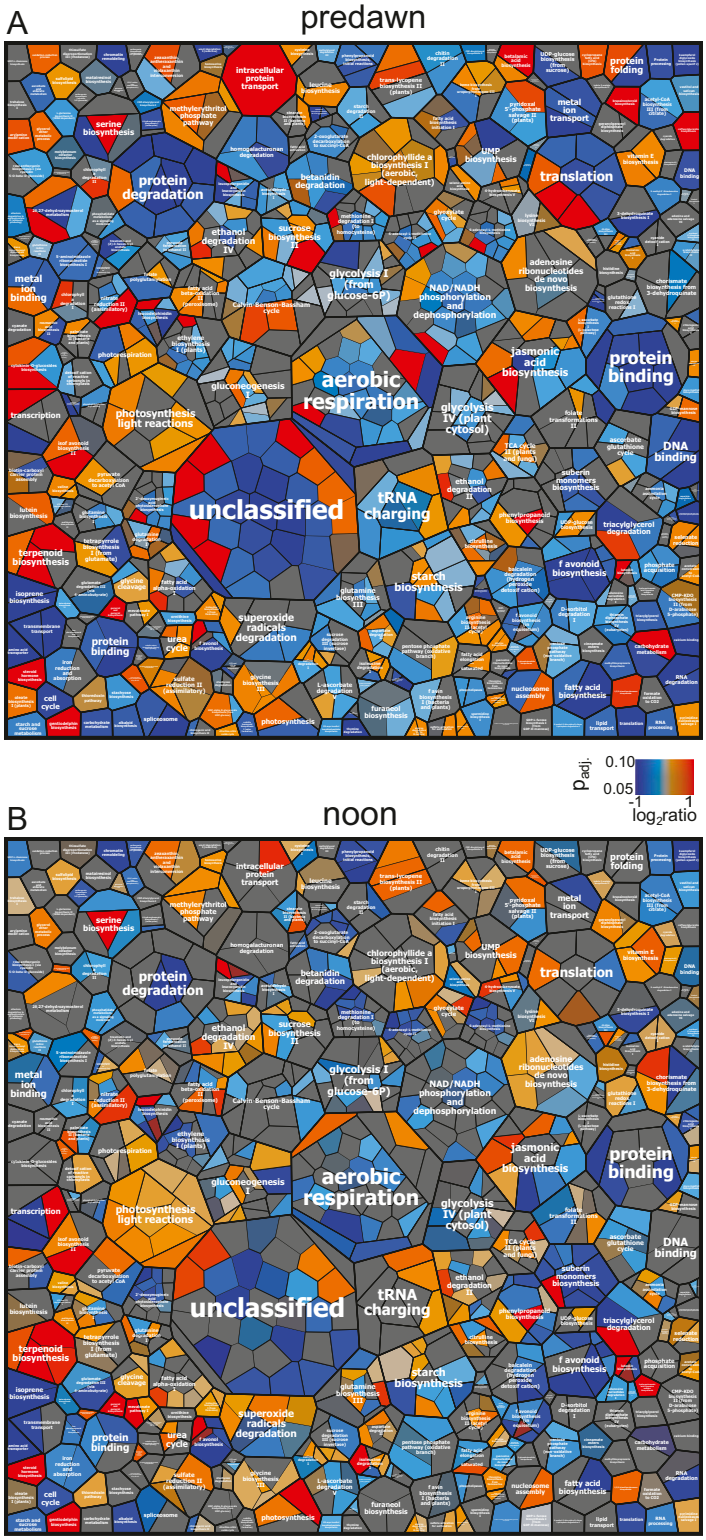

Fig. 5. (*A* and *B*) Voronoi Treemaps showing the overall proteome changes of IE and IR leaves. The total area of each map is subdivided into main categories, then the main categories into subcategories, and the subcategories into equally sized cells representing significantly changed proteins. Protein expression changes are displayed according to their functional categories and log2 ratios for IR/IE and are color coded: red, increased ratios; gray, unchanged ratios; and blue, decreased ratios. All measurements were made on separate trees for each genetic type and plantation as described in the main text.

Downloaded at UNIVERSITY OF ARIZONA on January 8, 2020

used to transform *A. tumefaciens* by electroporation. The final transformation of *P.* x *canescens* with both constructs was conducted as described by Meilan and Ma (56). Regenerated plantlets were PCR verified (*SI Appendix*, section S1) and maintained on media without antibiotics. Wild-type control and transgenic lines were amplified by micropropagation on half-concentrated Murashige and Skoog (MS) medium (57). Eight-week-old rooted shoots were transferred to small pots containing commercial potting soil and used for molecular screening.

Isoprene emission potential of transformants was initially assessed by measuring headspace isoprene accumulation in 8-wk-old rooted in vitro cultures (*SI Appendix*, section S1). From these efforts, 18 transformant genotypes were ultimately selected for further clonal propagation. Bulk propagation of this transgenic material was done by a commercial facility (Broadacres Nursery, Hubbard, OR) via clonal propagation of both dormant and green (actively growing) cuttings in a greenhouse. Bare stem cuttings from these greenhouse-grown transformants were the ultimate source of all subsequent field-planting stock. The wild-type CN and EV control lines were shown to retain relatively high rates of isoprene emission, whereas the transformed RNAi lines (IR) were shown to emit various rates of reduced isoprene emission, ranging to near-negligible levels.

Field Sites. The Oregon plantation was located on the grounds of Oregon State University's Peavy Arboretum (44.659° latitude N, 123.235° longitude W). The Arizona plantation was located on the grounds of the University of Arizona's Biosphere 2 campus near Oracle, AZ (32.344° latitude N, 110.510° longitude W). See *SI Appendix*, section S2, for further details of the plantations.

Measurement of Biomass Production and Leaf Gas Exchange Rates. At the completion of the field trail at the Oregon plantation, and before the initiation of spring-bud break the following year, whole trees were harvested and weighed for total biomass. Aboveground stems were coppiced and the root ball for each tree was removed with a miniexcavator and washed of all soil and debris. All tissues were subsequently dried at 60 C for 6 d in a large-capacity wood-drying convection kiln (Oregon State University School of Forestry), before weighing on a high-capacity balance (Mettler Toledo; MS12001L). In the Arizona plantation, trees were coppiced, dried, and weighed in December at the end of each growing season, for successive-year determination of aboveground biomass. Harvested, leafless stems were dried at room temperature for 6 wk, before weighing on a high-capacity balance (Sartorius; model LA 3400). For the Arizona trees, the crown stool and roots were excavated for 5 representative trees of each of the 4 genetic lines at the end of the 4-y growth period for determination of total nonshoot biomass (see *SI Appendix*, section S3 for details).

Isoprene emission rates and net CO_2 assimilation rates were measured at both plantation sites using a portable photosynthesis system for leaf CO_2/H_2O gas exchange (LiCor Inc.; model 6400) equipped with the broadleaf cuvette (6 cm^2) including the LED light system set for leaf temperature between 27 and 30 °C, light level of 1,800 μmol $m^{-2}{\cdot}s^{-1}$ PPFD, and chamber CO_2 mole fraction set to 400 μmol·mol^{-1} (25). In the Arizona studies, the gas-exchange system was connected to a chemiluminescence fast isoprene sensor (FIS) (Hills Scientific) for measurement of cuvette isoprene concentrations. A flow of O_3 to the reaction cell of the FIS was used to provide the oxidant needed to elicit a chemiluminescent reaction with isoprene, and photon counts were detected and converted to isoprene concentration using calibrations against a diluted standard tank (5 μmol·mol^{-1}; Airgas Inc.). In the Oregon studies, gas aliquots from the gas-exchange system chamber were analyzed for isoprene concentration by direct injection onto a gas chromatograph with a reducing gas detector (GC-RGD) (Peak Performer 1; Peak Laboratories LLC). The system was calibrated using gas-phase dilutions of standard isoprene (99%; Sigma Aldrich).

Proteome Measurements. One fully developed leaf was cut from each of 12 trees of each genotype on July 3, 2013 at the Arizona plantation and immediately frozen in liquid nitrogen prior to dawn (0415 to 0530 hours) and at midday (1200 to 1400 hours). Frozen leaves were homogenized and 50 mg leaf powder of 3 plants from each genotype was pooled for analysis, resulting in 4 replicates per genotype per harvest time. Samples were extracted and prepared for analysis as described in *SI Appendix*, section S7. Subsamples of 10 μg were subjected to filter-aided sample preparation (FASP) (58). LC-MSMS analysis of each individual subsample was performed on a Q Exactive HF mass spectrometer (ThermoFisher Scientific) online coupled to an Ultimate 3000 nano-RSLC (Dionex). Tryptic peptides were separated in a nonlinear acetonitrile gradient over 85 min on a C18 analytical column (nanoEase MZ HSS T3 Column, 100 Å, 1.8 μm, 75 μm × 250 mm; Waters). Precursor and TOP10 fragment spectra were acquired in the Orbitrap mass detector at 60,000× or 15,000× resolution, respectively. Generated raw files containing all acquired spectra were loaded to the Progenesis QI for proteomics software (v3.0; Nonlinear Dynamics Ltd., part of Waters) for′ label-free quantification and analyzed as previously described (59, 60). Features of only 1 charge or features with more than 7 charges were excluded. The raw abundances of the remaining features were normalized to allow for the correction of factors resulting from experimental variation. All MS/MS spectra were exported as MASCOT generic files and used for identification by the Mascot search engine (v 2.5.1; Matrix Science) in a *Populus trichocarpa* protein database (v3; 30,197,159 residues; 73,016 sequences). The search parameters were 10 ppm peptide mass and 0.02 Da MS/MS tolerance, with one missed cleavage allowed. For the identification and quantification of the leaf proteins, carbamidomethylation was set as a fixed modification and methionine oxidation and deamination of asparagine/glutamine as variable modification. A MASCOT-integrated decoy database search calculated a FDR of 0.45%, applying the MASCOT Percolator algorithm to distinguish between correct and incorrect spectrum identifications (61). The peptide assignments were reimported into the Progenesis QI software. After summing up the abundances of all unique peptides that were allocated to each protein, the identification and quantification results were exported. Voronoi Treemaps as introduced by Bernhardt et al. (62) were used to visualize the proteomics results. The Voroni Treemaps subdivide the 2D plane into subsections according to the hierarchical data structure of gene functional assignments as taken from the corresponding *A. thaliana* orthologs, which were obtained from the POPGENIE database (http://www.popgenie.org).

ACKNOWLEDGMENTS. R.K.M. acknowledges financial support from the Macrosystems Program in the Emerging Frontiers Section of the NSF (Award 1065790), the Ecosystems Program in the Division of Environmental Biology (NSF Award 1754430), and the Water, Environmental, and Energy Solutions program supported by the Technology and Research Initiative Fund from the State of Arizona. J.-P.S. acknowledges financial support from the German Ministry of Education and Research project (0315412). T.N.R. acknowledges financial support from Portland General Electric and Portland State University. S.H.S. acknowledges financial support from the US Department of Agriculture National Institute of Food and Agriculture (2013-67009-21008) and the Tree Biosafety and Genomics Research Cooperative at Oregon State University.

1. A. Limayem, S. C. Ricke, Lignocellulosic biomass for bioethanol production: Current perspectives, potential issues and future prospects. *Pror. Energy Combust. Sci.* **38**, 449–467 (2012).
2. I. Porth, Y. A. El-Kassaby, Using *Populus* as a lignocellulosic feedstock for bioethanol. *Biotechnol. J.* **10**, 510–524 (2015).
3. M. J. Stolarski *et al.*, Lignocellulosic biomass from short rotation woody crops as a feedstock for second-generation bioethanol production. *Ind. Crops Prod.* **75**, 66–75 (2015).
4. A. B. Guenther *et al.*, The model of emissions of gases and aerosols from nature version 2.1 (MEGAN2.1): An extended and updated framework for modeling biogenic emissions. *Geosci. Model Dev.* **5**, 1471–1492 (2012).
5. J. D. Fuentes *et al.*, Biogenic hydrocarbons in the atmosphere boundary layer: A review. *Bull. Am. Meteorol. Soc.* **81**, 1537–1575 (2000).
6. J. Lelieveld, P. Crutzen, F. Dentener, Changing concentration, lifetime and climate forcing of atmospheric methane. *Tellus Ser. B* **50**, 128–150 (1998).
7. N. Poisson, M. Kanakidou, P. J. Crutzen, Impact of non-methane hydrocarbons on tropospheric chemistry and the oxidizing power of the global troposphere: Three-dimensional modelling results. *J. Atmos. Chem.* **36**, 157–230 (2000).
8. A. Arneth *et al.*, From biota to chemistry and climate: Towards a comprehensive description of trace gas exchange between the biosphere and atmosphere. *Biogeosciences* **7**, 121–149 (2010).
9. K. Ashworth, O. Wild, C. N. Hewitt, Impacts of biofuel cultivation on mortality and crop yields. *Nat. Clim. Chang.* **3**, 492–496 (2013).
10. K. Ashworth, O. Wild, A. S. D. Eller, C. N. Hewitt, Impact of biofuel poplar cultivation on ground-level ozone and premature human mortality depends on cultivar selection and planting location. *Environ. Sci. Technol.* **49**, 8566–8575 (2015).
11. Food and Agricultural Organization (FAO), Livestock, Crop and Fertilizer Data (Food and Agricultural Organization of the United Nations: Statistics Division, 2015). http://www.fao.org/faostat/en/#data/QD. Accessed 10 December 2019.
12. S. J. Silva *et al.*, Impacts of current and projected oil palm plantation expansion on air quality over Southeast Asia. *Atmos. Chem. Phys.* **16**, 10621–10635 (2016).
13. J. A. Pyle *et al.*, The impact of local surface changes in Borneo on atmospheric composition at wider spatial scales: Coastal processes, land-use change and air quality. *Philos. Trans. R. Soc. Lond. B Biol. Sci.* **366**, 3210–3224 (2011).
14. K. Behnke *et al.*, Isoprene emission-free poplars–A chance to reduce the impact from poplar plantations on the atmosphere. *New Phytol.* **194**, 70–82 (2012).
15. F. Loreto, J.-P. Schnitzler, Abiotic stresses and induced BVOCs. *Trends Plant Sci.* **15**, 154–166 (2010).
16. M. Haworth *et al.*, Physiological responses of *Arundo donax* ecotypes to drought: A common garden study. *Glob. Change Biol. Bioenergy* **9**, 132–143 (2017).

Downloaded at UNIVERSITY OF ARIZONA on January 8, 2020

17. A. S. D. Eller, J. de Gouw, M. Graus, R. K. Monson, Variation among different genotypes of hybrid poplar with regard to leaf volatile organic compound emissions. *Ecol. Appl.* **22**, 1865–1875 (2012).
18. K. Behnke *et al*., Transgenic, non-isoprene emitting poplars don't like it hot. *Plant J.* **51**, 485–499 (2007).
19. K. Behnke *et al*., RNAi-mediated suppression of isoprene biosynthesis in hybrid poplar impacts ozone tolerance. *Tree Physiol.* **29**, 725–736 (2009).
20. K. Behnke *et al*., RNAi-mediated suppression of isoprene emission in poplar transiently impacts phenolic metabolism under high temperature and high light intensities: A transcriptomic and metabolomic analysis. *Plant Mol. Biol.* **74**, 61–75 (2010).
21. E. Vanzo *et al*., Facing the future: Effects of short-term climate extremes on isoprene-emitting and non-emitting poplar. *Plant Physiol.* **169**, 560–575 (2015).
22. T. N. Rosenstiel, M. J. Potosnak, K. L. Griffin, R. Fall, R. K. Monson, Increased CO2 uncouples growth from isoprene emission in an agriforest ecosystem. *Nature* **421**, 256–259 (2003).
23. D. A. Way, J.-P. Schnitzler, R. K. Monson, R. B. Jackson, Enhanced isoprene-related tolerance of heat- and light-stressed photosynthesis at low, but not high, CO_2 concentrations. *Oecologia* **166**, 273–282 (2011).
24. M. J. Potosnak, L. Lestourgeon, O. Nunez, Increasing leaf temperature reduces the suppression of isoprene emission by elevated CO_2 concentration. *Sci. Total Environ.* **481**, 352–359 (2014).
25. R. K. Monson *et al*., Interactions between temperature and intercellular CO_2 concentration in controlling leaf isoprene emission rates. *Plant Cell Environ.* **39**, 2404–2413 (2016).
26. A. T. Lantz *et al*., Isoprene suppression by CO_2 is not due to Triose Phosphate Utilization (TPU) limitation. *Front. For. Global Change* **2**, 8 (2019).
27. A. C. Ryan *et al*., Isoprene emission protects photosynthesis but reduces plant productivity during drought in transgenic tobacco (*Nicotiana tabacum*) plants. *New Phytol.* **201**, 205–216 (2014).
28. T. D. Sharkey, R. K. Monson, The future of isoprene emission from leaves, canopies and landscapes. *Plant Cell Environ.* **37**, 1727–1740 (2014).
29. B. A. Logan, T. J. Anchordoquy, R. K. Monson, R. S. Pan, The effect of isoprene on the properties of spinach thylakoids and phosphatidylcholine liposomes. *Plant Biol.* **1**, 602–606 (1999).
30. C. M. Harvey, Z. Li, H. Tjellström, G. J. Blanchard, T. D. Sharkey, Concentration of isoprene in artificial and thylakoid membranes. *J. Bioenerg. Biomembr.* **47**, 419–429 (2015).
31. E. Vanzo *et al*., Modulation of protein S-nitrosylation by isoprene emission in poplar. *Plant Physiol.* **170**, 1945–1961 (2016).
32. Z. Zuo *et al*., Isoprene acts as a signaling molecule in gene networks important for stress responses and plant growth. *Plant Physiol.* **180**, 124–152 (2019).
33. E. L. Singsaas, M. Lerdau, K. Winter, T. D. Sharkey, Isoprene increases thermotolerance of isoprene-emitting species. *Plant Physiol.* **115**, 1413–1420 (1997).
34. J. Peñuelas, J. Llusia, D. Asensio, S. Munne-Bosch, Linking isoprene with plant thermotolerance, antioxidants and monoterpene emissions. *Plant Cell Environ.* **28**, 278–286 (2005).
35. H. P. Affek, D. Yakir, Protection by isoprene against singlet oxygen in leaves. *Plant Physiol.* **129**, 269–277 (2002).
36. C. E. Vickers *et al*., Isoprene synthesis protects transgenic tobacco plants from oxidative stress. *Plant Cell Environ.* **32**, 520–531 (2009).
37. V. Velikova, F. Loreto, On the relationship between isoprene emission and thermotolerance in *Phragmites australis* leaves exposed to high temperatures and during the recovery from a heat stress. *Plant Cell Environ.* **28**, 318–327 (2005).
38. M. Haworth *et al*., Moderate drought stress induces increased foliar dimethylsulphoniopropionate (DMSP) concentration and isoprene emission in two contrasting ecotypes of *Arundo donax*. *Front. Plant Sci.* **8**, 1016 (2017).
39. T. D. Sharkey, Effects of moderate heat stress on photosynthesis: Importance of thylakoid reactions, rubisco deactivation, reactive oxygen species, and thermotolerance provided by isoprene. *Plant Cell Environ.* **28**, 269–277 (2005).
40. C. E. Vickers, J. Gershenzon, M. T. Lerdau, F. Loreto, A unified mechanism of action for volatile isoprenoids in plant abiotic stress. *Nat. Chem. Biol.* **5**, 283–291 (2009).
41. M. Kaling *et al*., UV-B mediated metabolic rearrangements in poplar revealed by non-targeted metabolomics. *Plant Cell Environ.* **38**, 892–904 (2015).
42. N. R. Street *et al*., The genetics and genomics of the drought response in *Populus*. *Plant J.* **48**, 321–341 (2006).
43. C. M. Harvey, T. D. Sharkey, Exogenous isoprene modulates gene expression in unstressed *Arabidopsis thaliana* plants. *Plant Cell Environ.* **39**, 1251–1263 (2016).
44. M. Tattini *et al*., Isoprene production in transgenic tobacco alters isoprenoid, non-structural carbohydrate and phenylpropanoid metabolism, and protects photosynthesis from drought stress. *Plant Cell Environ.* **37**, 1950–1964 (2014).
45. V. Velikova *et al*., Genetic manipulation of isoprene emissions in poplar plants remodels the chloroplast proteome. *J. Proteome Res.* **13**, 2005–2018 (2014).
46. A. Ghirardo *et al*., Metabolic flux analysis of plastidic isoprenoid biosynthesis in poplar leaves emitting and nonemitting isoprene. *Plant Physiol.* **165**, 37–51 (2014).
47. FAO, Poplars and other fast-growing trees -renewable resources for future green economies. Synthesis of Country Progress Reports. *25th Session of the International Poplar Commission*. http://www.fao.org/3/a-mt504e.pdf. Accessed 10 December 2019.
48. FAO, Synthesis of country progress reports: Activities related to poplar and willow cultivation and utilization, 2000 through 2003. http://www.fao.org/forestry/13363-0a6ec625ad5b96bb7c6565fb0c3660d9.pdf. Accessed 10 December 2019.
49. C. Wiedinmyer, X. X. Tie, A. B. Guenther, R. Neilson, C. Granier, Future changes in biogenic isoprene emissions: How might they affect regional and global atmospheric chemistry? *Earth Interact.* **10**, 1–19 (2006).
50. A. G. Carlton, C. Wiedinmyer, J. H. Kroll, A review of secondary organic aerosol (SOA) formation from isoprene. *Atmos. Chem. Phys.* **9**, 4987–5005 (2009).
51. C. E. Scott *et al*., Impact on short-lived climate forcers (SLCFs) from a realistic land-use change scenario via changes in biogenic emissions. *Faraday Discuss.* **200**, 101–120 (2017).
52. K. H. Bates, D. J. Jacob, A new model mechanism for atmospheric oxidation of isoprene: Global effects on oxidants, nitrogen oxides, organic products, and secondary organic aerosol. *Atmos. Chem. Phys.* **19**, 9613–9640 (2019).
53. W. H. Chen *et al*., Regional to global biogenic isoprene emission responses to changes in vegetation from 2000 to 2015. *J. Geophy. Res. Atmos.* **123**, 3757–3771 (2018).
54. S. H. Strauss, A. Costanza, A. Séguin, BIOTECHNOLOGY. Genetically engineered trees: Paralysis from good intentions. *Science* **349**, 794–795 (2015).
55. J. D. Wolt, K. Wang, B. Yang, The regulatory status of genome-edited crops. *Plant Biotechnol. J.* **14**, 510–518 (2016).
56. R. Meilan, C. Ma, Poplar (*Populus* spp.). *Methods Mol. Biol.* **344**, 143–151 (2006).
57. J. C. Leplé, A. C. M. Brasileiro, M. F. Michel, F. Delmotte, L. Jouanin, Transgenic poplars: Expression of chimeric genes using four different constructs. *Plant Cell Rep.* **11**, 137–141 (1992).
58. J. R. Wiśniewski, A. Zougman, N. Nagaraj, M. Mann, Universal sample preparation method for proteome analysis. *Nat. Methods* **6**, 359–362 (2009).
59. S. M. Hauck *et al*., Deciphering membrane-associated molecular processes in target tissue of autoimmune uveitis by label-free quantitative mass spectrometry. *Mol. Cell. Proteomics* **9**, 2292–2305 (2010).
60. J. Merl, M. Ueffing, S. M. Hauck, C. von Toerne, Direct comparison of MS-based label-free and SILAC quantitative proteome profiling strategies in primary retinal Müller cells. *Proteomics* **12**, 1902–1911 (2012).
61. M. Brosch, L. Yu, T. Hubbard, J. Choudhary, Accurate and sensitive peptide identification with Mascot Percolator. *J. Proteome Res.* **8**, 3176–3181 (2009).
62. J. Bernhardt, S. Funke, M. Hecker, J. Siebourg, "Visualizing gene expression data via Voronoi Treemaps" in *2009 6th International Symposium on Voronoi Diagrams*, F. Anton, Ed. (IEEE, Copenhagen, Denmark, 2009), pp. 233–241.

Downloaded at UNIVERSITY OF ARIZONA on January 8, 2020